Biologikum Weihenstephan

Fachgebiet für Entwicklungsbiologie der Pflanzen

Technische Universität München

Characterization of STRUBBELIG, an Atypical Receptor-Like Kinase, and Components of its Signaling Pathway in *Arabidopsis*

Martine Batoux

Vollständiger Abdruck der von der Fakultät

Wissenschaftszentrum Weihenstephan für Ernährung, Landnutzung und Umwelt

der Technischen Universität München

zur Erlangung des akademischen Grades eines

Doktors der Naturwissenschaften (Dr. rer. nat.)

genehmigten Dissertation.

Vorsitzender:		Univ-Prof. Dr. Erwin Grill
Prüfer der Dissertation:	1.	Univ-Prof. Dr. Kay H. Schneitz
	2.	Univ-Prof. Dr Alfons Gierl

Die Dissertation wurde am 12. Februar 2007 bei der Technischen Universität München eingereicht und durch die Fakultät Wissenschaftszentrum Weihenstephan für Ernährung, Landnutzung und Umwelt am 20. März 2007 angenommen.

Table of Contents

SUMMARY

In multicellular organisms, development relies on communication between cells. Cell communication is achieved thanks to receptors. Receptor-like kinases (RLKs) are a prominent group of receptors in plants. In *Arabidopsis*, certain of RLKs, such as CLAVATA1, ERECTA and BRASSINOSTEROID INSENSITIVE1, are known to have important roles in plant development. STRUBBELIG (SUB) is a new RLK necessary for plant development. Plants with a defect in SUB present alterations in the organ shape and size.

To understand better the function of *SUB*, mutations, affecting different structural domains of the SUB protein, were identified and the phenotype of the alleles analysed. In a L*er* background, phenotypic features and strength were similar in five different *sub* alleles. Moreover, a site-directed mutagenesis approach indicates that the kinase activity of SUB is not required for its biological function. Indeed, expression of several SUB variants with altered amino acids that are important for ATP binding can rescue *sub-1* phenotype.

The *SUB* expression pattern was investigated by the generation of transgenic plants expressing the *GUS* gene under the control of *SUB* regulatory elements. *GUS* activity was detected in mitotic active tissues: shoot apical and floral meristems, lateral organ primordia (root, leaves and floral organ) and in the developing vascular system. These results point out a role for SUB in proliferating tissues.

To elucidate the function of SUB, seventeen SUB putatitive interacting partners were identified through a yeast two-hybrid screen with the SUB intracellular domain. SUB interacts in the yeast system with proteins usually involved in other RLK pathways, proteins implied in signaling pathways and proteins putative interacting with the cytoskeleton. On the basis of their very similar expression patterns, the interaction of SUB with one of the candidates, ALADIN, a putative nucleoporin, was further analysed and it could be shown that SUB and ALADIN can also interact *in vitro*.

ZUSAMMENFASSUNG

Die Kommunikation zwischen Zellen ist wichtig für die Entwicklung multizellulärer Organismen. Diese Zellkommunikation wird durch Rezeptoren ermöglicht. Rezeptorkinasen (RLKs) sind eine wichtige Gruppe von Rezeptoren in Pflanzen. Einige RLKs, wie zum Beispiel CLAVATA1, ERECTA oder BRASSINOSTEROID INSENSITIVE1, spielen eine wichtige Rolle in der pflanzlichen Entwicklung. STRUBBELIG (SUB) ist eine neue RLK mit einer wichtigen Funktion in der Organogenese. Entsprechende Mutanten zeigen einen Defekt in der Organgrösse und Organform.

Um ein besseres Verständnis der Funktion von *SUB* zu erhalten wurden verschiedene Mutationen, welche spezifische strukurelle Domänen des SUB-Proteins betreffen, identifiziert und der Phänotyp der Allele analysiert. Im L*er* Hintergrund führten fünf verschiedene *sub* Allele zu einem sehr ähnlichen mutanten Phänotyp. Zusätzlich wurde mittels “site-directed mutagenesis”-Ansätzen gezeigt, dass SUB keine Kinaseaktivität für seine biologische Funktion benötigt. Die Expression von mehreren SUB-Varianten, die durch Veränderungen in der ATP-bindenden Stelle gekennzeichnet waren, führte zu einer Rettung des *sub-1* Phänotyps.

Das Expressionsmuster von *SUB* wurde mittels transgener Reporterlinien analysiert. Die transgenen Pflanzen trugen ein *GUS*-Gen dessen Expression von regulatorischen Sequenzen des *SUB*-Promoters gesteuert wurde. GUS-Aktivität konnte in mitotisch-aktivem Gewebe detektiert werden: im Sprossmeristem und Blütenmeristem, in Primordien der lateralen Organe und im sich entwickelnden vaskulären Gewebe. Diese Befunde stützen die Idee, dass *SUB* eine Rolle in proliferierenden Zellen spielt.

Um die Funktion von SUB weiter zu studieren wurden mittels eines “yeast two-hybrid screens” 17 Proteine identifiziert, die möglicherweise an die intrazelluläre Domäne von SUB binden können. In diesem System interagiert SUB mit Proteinen die oft auch in anderen RLK-Signalketten involviert sind, mit generellen Signalkettenproteinen und mit Proteinen die eine mögliche Verbindung zum Zytoskelett darstellen könnten. Aufgrund entsprechender überlappender

Expressionsmuster wurde die Interaktion mit einem Kandidaten, ALADIN, einem möglichen Nukleoporin, weiter untersucht. Es konnte gezeigt werden, dass SUB und ALADIN auch *in vitro* interagieren können.

Chapter 1: Signaling in plant development

The plant embryo looks like a miniature seedling that lacks most of the adult plant organs. However, the embryo comprises the structures necessary to form the adult organism during post-embryogenesis: the shoot apical meristem (SAM) and the root apical meristem (RAM) (Walbot, 1996). The SAM gives rise to the aerial organs during vegetative (leaves) and reproductive phases (stem and flowers) while the RAM produces the underground organ, the root. Signaling pathways take an important place to coordinate post-embryogenic development. To build an adult plant, signaling pathways should attribute a particular fate to each cell. Moreover to achieve a harmonious plant, cell shape is also important. Here, pathways responsible for the fate and shape of plant cells will be descrcibed.

1-1 CELL FATE

1-1-1 Importance of cell position

A laser cell ablation approach was successful to understand whether cell fate depends on cell lineage or cell position, especially in the root. The root is composed of different tissues i.e. from the outside of the root, epidermis, cortex, endodermis, pericycle and vascular bundle. Cell lineage of the root originates from stem cells called initial cells. Different type of initial cells could be identified: epidermal, cortical, central root cap/columnella and pericycle/vascular tissue initials (Dolan *et al.*, 1993). Anticlinal divisions of initials give rise to daughter cells. Then, daughter cells are subjected to a periclinal division. By this way, epidermal and cortical initials originate the root cap/epidermis and the cortex/endodermis, respectively (Scheres *et al.*, 1994). The reiteration of this cell division process leads to root growth. Is the fate of cells from the different tissue layers is due to their position or due to their belonging to the same cell file?

Van der Berg and colleagues (1995) describe that the ablation of an epidermal initial results in both, the reallocation of the neighboring cortex cell in the epidermis

cell file and the respecification of the former cortex cell. Indeed the former cortex cell undergoes a periclinal division that results in root cap and epidermis cells but not in cortex and endodermis cell. In the case of a cortical initial ablation, the invasion and respecification of an epidermis cell also occurs. In contrary, the ablation of three cortical daughter cells, resulting in the isolation of the cortical initial cell, generates the formation of a new cortical daughter cell. However, the new cell is unable to divide and form a cortex and endodermis cell. So, these cell ablation experiments demonstrate that fate is not depending of cell lineage but on cell-cell communication between cells in a distal and a radial direction (van den Berg *et al.*, 1995). SHORT ROOT (SHR), a transcription factor of the GRAS family was shown to be a determinant in radial signaling between stele and endodermis cells. SHR is required for endodermis fate (Nakajima *et al.*, 2001). Interestingly, *SHR* transcript is present only in the stele and not in the endodermis (Nakajima *et al.*, 2001). However, SHR protein is also localized in the first layer in contact with the stele (Sena *et al.*, 2004). SHR can move from cell to cell in a controlled manner. Indeed, a mutation in *SHR,* inhibiting the movement of SHR, suggests its transport via cell plasmodesmata (Gallagher *et al.*, 2004). By an unknown pathway, cortical cells also influence the epidermal cell fate, which are differentiating to non-hair cells and hair cells (Galway *et al.*, 1994).

1-1-2 Cell identity

The root cell epidermis is a good example where two neighboring cells acquire a different fate. The root epidermis is composed of two types of cells, hair cells (H-cells or trichoblasts) and non-hair cells (N-cells or atrichoblasts). H-cells preferentially originate from epidermis cells, which are positioned above two cortical cells. In contrast only one cortical cell underlies epidermis cells with a N-cell fate (Dolan *et al.*, 1993). Positional information from cortical cells may direct epidermis cell fate (Galway *et al.*, 1994). Epidermis cell differentiation is observable at the cellular level. H-cells are characterized by a reduced cell length, a denser cytoplasm and a deferred vacuolation (Dolan *et al.*, 1994; Galway *et al.*, 1994). By default, all epidermis cells are programmed for non-hair cell fate. However, this program is suppressed in H-cells

in a non-cell autonomous fashion. In N-cells, a complex composed of a MYB protein, WEREWOLF (WER; Lee and Schiefelbein, 1999), a WD-repeat protein TRANSPARENT TESTA GLABRA (TTG; Galway *et al.*, 1994) and two bHLH proteins GLABRA3 (GL3; Bernhardt *et al.*, 2003) and ENHANCER OF GLABRA3 (EGL3; Bernhardt *et al.*, 2003) may promote the expression of a homeodomain-leucine zipper gene *GLABRA2* (*GL2*; Di Cristina *et al.*, 1996; Masucci *et al.*, 1996). WER, GL3 and EGL3 can physically interact in a yeast two-hybrid system (Bernhardt *et al.*, 2003). WER and TTG can positively regulate *GL2* (Hung *et al.*, 1998; Lee and Schiefelbein, 1999). WER directly binds the promoter of *GL2* (Koshino-Kimura *et al.*, 2005) and can migrate from N-cells to H-cells but its molecular function in H-cells is not known (Ryu *et al.*, 2005).

In N-cells, WER also activates the expression of CAPRICE (CPC; Wada *et al.*, 1997), a R3-type Myb like protein, by binding directly the promoter of *CPC* (Ryu *et al.*, 2005; Koshino-Kimura *et al.*, 2005). *CPC* is strictly expressed in N-cells, but CPC is found in the nucleus of H-cells (Lee and Schiefelbein, 1999; Wada *et al.*, 2002). CPC is able to move to H-cells through plasmodesmata to repress *GL2* expression (Kurata *et al.*, 2005). In *cpc-1* background, the exclusive N-cell expression of *GL2* spreads into both types of epidermis cells (Lee and Schiefelbein, 1999). CPC specifies H-cell in concert with two other myb-related proteins, TRYPTYCHON, (TRY) and ENHANCER OF TRY AND CPC1 (ETC1). *TRY* and *ECT1* are strictly expressed in N-cells. Despite of no alteration in *try* and *etc1* root hairs, *try* and *etc1* aggravate the *cpc* phenotype (Schellmann *et al.*, 2002). In H-cells, CPC and TRY interact with GL3 and EGL3 (Bernhardt *et al.*, 2003; Zhang *et al.*, 2003).

GL2 is the last regulator of epidermis cell fate. Its activation in N-cells negatively regulates ethylene and auxin pathways (Masucci *et al.*, 1996). Ethylene and auxin are known to promote the extension of root hairs (Masucci and Schiefelbein, 1996). Repression in H-cells and activation in N-cells of GL2 seems also be controlled at the chromatin level in a cell position dependant manner. In N-cells and H-cells, the chromatin around the *GL2* locus presents an open and closed configuration, respectively. At the *GL2* locus, the chromatin state is directly regulated by FASCIATA2 (FAS), one of the three subunits of the chromatin assembly factor 1 CAF1; (Kaya *et al.*, 2001; Costa and Shaw, 2006). In *fas2*, both type of cells show an

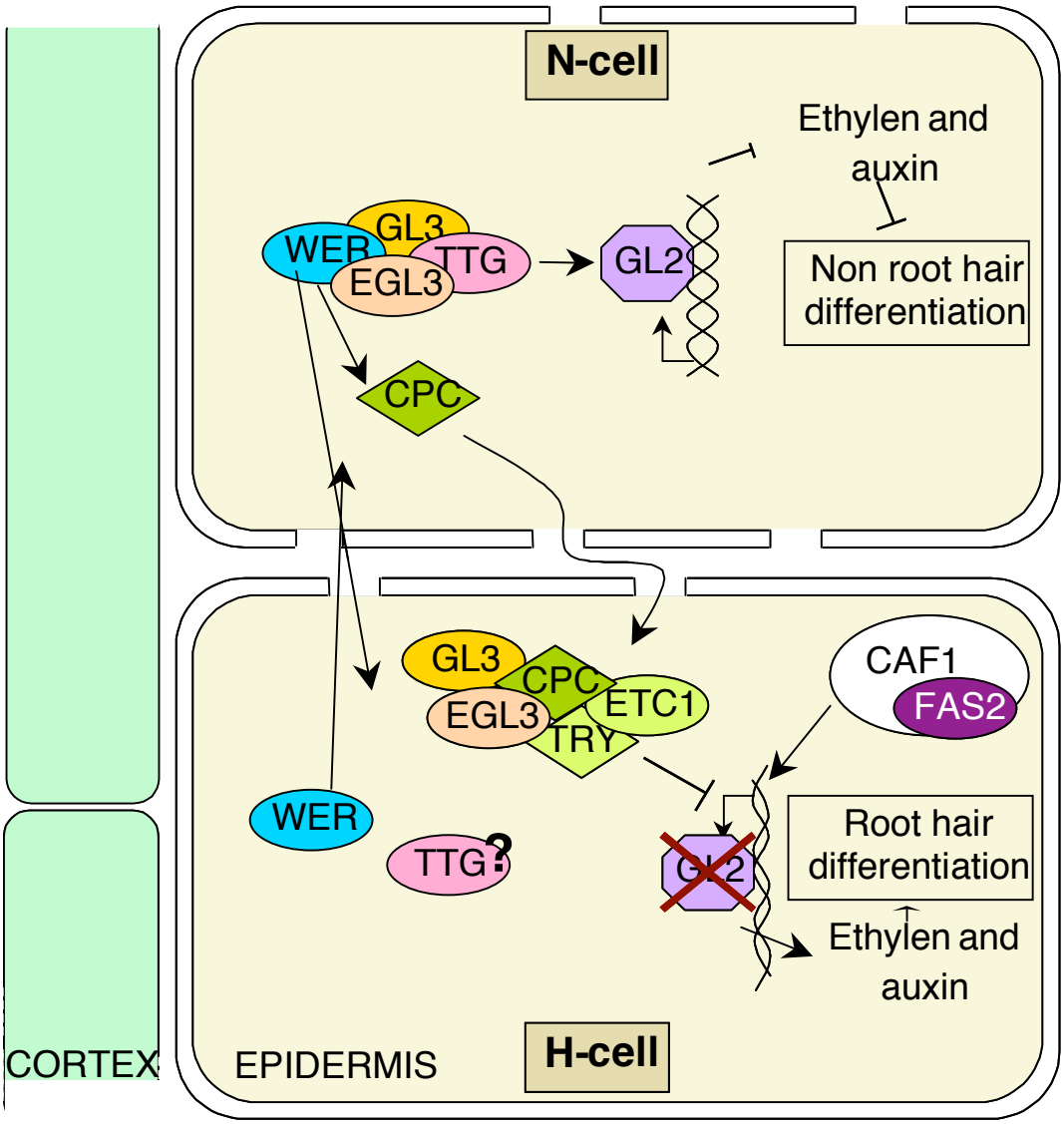

Figure 1-1. Model of root epidermis cell fate. Epidermis cells acquire root hair specification via positional information mediated by underlay cell layers (red spots between cortex and epidermis). SUB/SCM may propagate positional signaling in hair cell (H-cell), which results in the inhibition of the default non hair cell (N-cell) pathway. The N-cell pathway activates *GL2* expression via the WER-GL3-EGL3-TTG complex. GL2 may repress genes involved in auxin and ethylene pathways, which are key hormones of hair differentiation. In H-cell, SUB/SCM, activated by positional information, induces the repression of *WER*. So, the WER-GL3-EGL3-TTG complex is disrupted and allows formation of a new complex made of GL3-EGL3-CPC-TRY-ETC. The formation of this complex depends also on the migration of CPC from N-cell to H-cell through plasmodesmata. The new protein complex negatively regulates *GL2.* FAS2 may also repress *GL2* expression by remodeling and closing the chromatin at its locus. With *GL2* being inhibited, the auxin and ethylene pathways can promote the differentiation of root hairs.

opened state of *GL2* chromatin. So far no relationship between FAS2 and the other players of cell epidermis specification are established.

1-2 ORGAN SHAPE

In plants, the architecture of organs depends on different processes. Due to a rigid cell wall, plant cells do not migrate. So the orientation of the cell division plane will attribute the definitive position of the cell. At the end of cell division, the deposition of cell wall microfibrils and the organization of cytoskeletal elements are responsible for cell morphogenesis.

1-2-1 Cell division plan

In G2 phase of the cell cycle, the disposition of the preprophase band (PPB) is marking the future plane of cell division. The PPB is made of actin filaments and microtubules (MTs). At the beginning of mitosis, actin filaments are dispersed while the MTs participate in the formation of the spindle. During cytokinesis, at the same position, the phragmoplast will be formed (Smith, 2001). To conserve the exact position of the PPB for the formation of the cell plate, memory components should be present. AUXIN-INDUCED IN ROOT CULTURES9 (AIR9) may be involved in this process (Buschmann *et al.*, 2006).

Proteins with diverse roles can affect the position of the cell plate. A maize MT binding protein, TANGLED1 (TAN1), is known to be responsible for the PPB and phragmoplast position in leaf development (Smith *et al.*, 1996; Cleary and Smith, 1998). Two *Arabidopsis* related-kinesins, PHRAGMOPLAST ORIENTING KINESIN1 and 2 (POK1 and POK2) were found to interact with maize TANGLED1. In *Arabidopsis*, *pok1pok2* double mutants display misposition of cell plates as early as at the embryo octant stage (Muller *et al.*, 2006). POK1 and POK2 may interact with a TANGLED1 ortholog in *Arabidopsis* (ATN) to link the dividing nucleus to the cortex (Muller *et al.*, 2006). Another mutant, *root-shoot-hypocotyl-defective* (*rsh*) displays a misposition of the cell plate. *RSH* encodes a hydoxyprolin-rich glycoprotein. RSH is

located in the cell wall and may involved in the connection between the cell wall to the phragmoplast (Hall and Cannon, 2002). KNOLLE (KN), a cytokinesis-specific syntaxin, and a member of the SNARE family (soluble *N*-ethylmaleimide–sensitive factor attachment protein receptor), takes part of the formation of the cell plate. KN allows the fusion of endocytosis vesicles to the cell plate (Dhonukshe *et al.*, 2005). KN binds *in vitro* to KEULE (KEU), a SEC1 related protein, and necessary for specific interaction between SNARE proteins (Assaad *et al.*, 2001). *kn* and *keu* show an incomplete cell wall between two daughter cells due to the non-fusion of cell plate-forming vesicles (Lukowitz *et al.*, 1996; Waizenegger *et al.*, 2000).

1-2-2 Cell elongation

1-2-2-1 Microfibrils deposition in the cell wall

The deposition of the cell wall is responsible for the shape of the cell during the expansion phase. Microscopic observations of the microfibril and MT orientation showed that these two structures are perpendicular to each other and MTs may be responsible for the orientation of the microfibrils (Wasteneys and Fujita, 2006). Recently, MTs were found to have an influence on the distribution and the guidance of cellulose synthase (Paredez *et al.,* 2006). COBRA (COB) is another protein, which may associate the microfibril orientation to the one of MTs. The microfibrils of *cob* are disordered, and the cells show radial rather longitudinal elongation. COB is a glycosylphosphatidylinositol (GPI)-anchored protein, which may be responsible for the microfibril deposition in a MT dependant-manner. Indeed, the depolymeristion of MTs induces a mislocation of COB (Roudier *et al.*, 2005; Wasteneys and Fujita, 2006).

1-2-2-2 Cortical microtubule array

The cortical MT array takes part in directing plant growth. Alteration on the MTs network i.e. tubulin or MTs associated-proteins (MAPs) affect the growth of the plant. MTs composed of mutated TUBULINA6/4 generate a left-handed helical growth. The petiols, petals, rosette leaves, flowers, hypocotyl and root of the corresponding mutant, *lefty*, are twisted (Thitamadee *et al.*, 2002).

Contrary to *lefty*, two mutants altered in *MAPs* genes, *SKU6/SPIRAL1* (*SPR1*) and *SPR2 /TORTIFOLIA* (*TOR*) display a right-handed growth (Furutani *et al.*, 2000; Nakajima *et al.*, 2004; Shoji *et al.*, 2004). SKU6/SPR1 is preferentially localized at the minus end of MTs and may regulate the growth of the minus end (Nakajima *et al.*, 2004). SPR2/TOR encodes for a member of a HEAT-repeat-containing family. SPR2/TOR can bind MTs *in vitro* and *in vivo* (Shoji *et al.*, 2004).

So far, the two different classes of mutants, with right- or left-handed helical growth, are not well understood. The destabilization of cortical MTs network can lead to a random orientation (Abe *et al.*, 2004).

1-3 STRUBBELIG, A RECEPTOR LIKE-KINASE INVOLVED IN PLANT DEVLOPMENT

Since the sequencing of the *Arabidopsis* genome (Arabidopsis Genome Initiative, 2000), a lot of RLK genes were characterized and their function elucidated. However, the function of certain genes is not well understood. This is the case for STRUBBELIG (SUB).

1-3-1 Phenotype of sub

The s*ub* pleiotropic phenotype indicates an important role of SUB in plant development, especially cell proliferation, cell morphogenesis and cell division. Mutations in *SUB* were isolated in an EMS screen based on female sterility (Schneitz *et al.*, 1997). Indeed, *sub* displays semi-sterility mainly due to an altered proliferation of the ovule outer integument and to the frequent absence of the embryo sac

(Chevalier *et al.*, 2005). Moreover, *sub* has a smaller plant size than WT and the stem, carpels and petal pedicels are twisted. Contrary to twisted mutants known so far (see section 1-3-2-2), the *sub* twisting is irregular i.e. does not follow a particular helical growth. Another feature of *sub* is a reduction in cell numbers of the epidermal, cortex and pith of the stem. Finally, the L2 layer of the young *sub* flower meristem shows an elevated frequency of periclinal cell divisions (Chevalier *et al.*, 2005).

1-3-2 SUB, a receptor like-kinase (RLK)

SUB was cloned and identified by a map-based approach (gene identifier At1g11130). The predicted protein encodes a RLK of 748 amino acids (AA) with an estimated molecular weight of 84,5 kDa. The extracellular domain of SUB is composed of a signal peptide, the SUB domain, six leucine rich repeats (LRR), a proline-rich region containing two PEST sequences (Rechsteiner and Rogers, 1996), a single spanning transmembrane domain, an intracellular made of a juxta-membrane and a kinase domains. SUB protein is located in the plasma membrane (Ram Kishor Yadav, unpublished data). Interestingly, the *SUB* mRNA pattern differs from the SUB protein localization. For example, *SUB* expression is found in all SAM cell layers whereas SUB protein is restricted to the L3. In the cell division zone of root, *SUB* mRNA is present in all tissue layers while SUB is present only in the stele. *SUB* expression seems to be post-translationally regulated (Ram Kishor Yadav, unpublished data).

SUB is a member of LRR-V class of RLKs (Shiu and Bleecker, 2001). The eight other members of the family were called *STRUBBELIG RECEPTORS FAMILY 1-8* (*SRF1-8*). So far, only a function was attributed to *SRF4*. *SRF4* play a role on the leaf size. Indeed, *srf4* loss-of-function mutants present smaller rosette leaves than WT, while *SRF4* gain-of-function mutants show bigger leaves than WT (Eyueboglu *et al.*, submitted paper).

1-3-3 Role of SUB in root epidermis cell fate

SUB, also known as SCRAMBLED (SCM) has been shown to participate in the specification of root epidermis cells (Kwak *et al.*, 2005; see section 1-2-2). The role of *SUB/SCM* in cell fate regulation in the root epidermis was discovered by altered *GL2* expression in a *sub/scm* mutant (Kwak *et al.*, 2005). The misexpression of GL2 leads to the formation of hair in H-cells as well in N-cells and the absence of hair in H-cells. In *sub/scm*, altered expression of *GL2*, but also *CPC*, *GL3* and *EGL3*, is due to the misregulation of *WER*, an upstream component of the epidermis cell fate pathway. The level of *WER* expression is higher in *cpc1sub/scm* comparing to *cpc1*, therefore *SUB/SCM* negatively regulate the expression of *WER* (Kwak and Schiefelbein, 2007). Moreover, *SUB* seems to be responsible for the mediation of positional information between the cortical and epidermis cell layers (Kwak and Schiefelbein, 2007).

1-3-4 SUB may act non-cell autonomously

The expression of *SUB* under the *AtML1* promoter could rescue all features of the *sub-1* phenotype. *AtML1* expression is restricted to the plant epidermis cell layer (Sessions *et al.*, 1999). Indeed, SUB was restricted to the L1 of the SAM although under *SUB* promoter, SUB is located in the L3. However the mislocation of SUB could still rescue the L2 periclinal cell division of *sub* young flowers meristem (Ram Yadav Kishor, unpublished data).

1-3-5 The aim of this work

To link the *sub* phenotype to a biological role of SUB, different strategies were used. First, a structure-function analysis of SUB protein was investigated. For this purpose, new alleles of *sub* were isolated and the role of certain AAs of SUB was investigated by site-directed mutagenesis (Chapter 2). The expression pattern of *SUB* was analyzed in detail via the generation of *SUB* promoter GUS reporter lines (Chapter 3).

Finally, a first set of proteins, potentially interacting proteins with SUB, were identified via a yeast two-hybrid approach (Chapter 4).

1-4 REFERENCES

Abe, T., Thitamadee, S. and Hashimoto, T. (2004). Microtubule defects and cell morphogenesis in the lefty1lefty2 tubulin mutant of arabidopsis thaliana. *Plant Cell Physiol*, **45**(2): 211-20.

Arabidopsis Genome Initiative (2000). Analysis of the genome sequence of the flowering plant *arabidopsis thaliana*. *Nature*, **408**(6814): 796-815.

Assaad, F. F., Huet, Y., Mayer, U. and Jurgens, G. (2001). The cytokinesis gene keule encodes a sec1 protein that binds the syntaxin knolle. *J Cell Biol*, **152**(3): 531-43.

Baskin, T. I. (2001). On the alignment of cellulose microfibrils by cortical microtubules: A review and a model. *Protoplasma*, **215**(1-4): 150-71.

Bernhardt, C., Lee, M. M., Gonzalez, A., Zhang, F., Lloyd, A. and Schiefelbein, J. (2003). The bhlh genes glabra3 (gl3) and enhancer of glabra3 (egl3) specify epidermal cell fate in the arabidopsis root. *Development*, **130**(26): 6431-9.

Buschmann, H., Chan, J., Sanchez-Pulido, L., Andrade-Navarro, M. A., Doonan, J. H. and Lloyd, C. W. (2006). Microtubule-associated air9 recognizes the cortical division site at preprophase and cell-plate insertion. *Curr Biol*, **16**(19): 1938-43.

Chevalier, D., Batoux, M., Fulton, L., Pfister, K., Yadav, R. K., Schellenberg, M. and Schneitz, K. (2005). STRUBBELIG defines a receptor kinase-mediated signaling pathway regulating organ development in arabidopsis. *PNAS*, **102**(25): 9074-9.

Cleary, A. L. and Smith, L. G. (1998). The tangled1 gene is required for spatial control of cytoskeletal arrays associated with cell division during maize leaf development. *Plant Cell*, **10**(11): 1875-88.

Costa, S. and Shaw, P. (2006). Chromatin organization and cell fate switch respond to positional information in arabidopsis. *Nature*, **439**(7075): 493-6.

Dhonukshe, P., Mathur, J., Hulskamp, M. and Gadella, T. W., Jr. (2005). Microtubule plus-ends reveal essential links between intracellular polarization and localized modulation of endocytosis during division-plane establishment in plant cells. *BMC Biol*, **3**: 11.

Di Cristina, M., Sessa, G., Dolan, L., Linstead, P., Baima, S., Ruberti, I. and Morelli, G. (1996). The arabidopsis athb-10 (glabra2) is an hd-zip protein required for regulation of root hair development. *Plant J*, **10**(3): 393-402.

Dolan, L., Duckett, C. M., Grierson, C., Linstead, P., Schneider, K., Lawson, E., Dean, C., Poethig, R. S. and Roberts, K. (1994). Clonal relationships and cell patterning in the root epidermis of arabidopsis. *Development*, **120**(9): 2465-2474.

Dolan, L., Janmaat, K., Willemsen, V., Linstead, P., Poethig, S., Roberts, K. and Scheres, B. (1993). Cellular organisation of the arabidopsis thaliana root. *Development*, **119**(1): 71-84.

REFERENCES

Dumais, J., Long, S. R. and Shaw, S. L. (2004). The mechanics of surface expansion anisotropy in medicago truncatula root hairs. *Plant Physiol*, **136**(2): 3266-75.

Furutani, I., Watanabe, Y., Prieto, R., Masukawa, M., Suzuki, K., Naoi, K., Thitamadee, S., Shikanai, T. and Hashimoto, T. (2000). The spiral genes are required for directional control of cell elongation in aarabidopsis thaliana. *Development*, **127**(20): 4443-53.

Gallagher, K. L., Paquette, A. J., Nakajima, K. and Benfey, P. N. (2004). Mechanisms regulating short-root intercellular movement. *Curr Biol*, **14**(20): 1847-51.

Galway, M. E., Masucci, J. D., Lloyd, A. M., Walbot, V., Davis, R. W. and Schiefelbein, J. W. (1994). The ttg gene is required to specify epidermal cell fate and cell patterning in the arabidopsis root. *Dev Biol*, **166**(2): 740-54.

Hall, Q. and Cannon, M. C. (2002). The cell wall hydroxyproline-rich glycoprotein rsh is essential for normal embryo development in arabidopsis. *Plant Cell*, **14**(5): 1161-72.

Hung, C. Y., Lin, Y., Zhang, M., Pollock, S., Marks, M. D. and Schiefelbein, J. (1998). A common position-dependent mechanism controls cell-type patterning and glabra2 regulation in the root and hypocotyl epidermis of arabidopsis. *Plant Physiol*, **117**(1): 73-84.

Kaya, H., Shibahara, K. I., Taoka, K. I., Iwabuchi, M., Stillman, B. and Araki, T. (2001). Fasciata genes for chromatin assembly factor-1 in arabidopsis maintain the cellular organization of apical meristems. *Cell*, **104**(1): 131-42.

Koshino-Kimura, Y., Wada, T., Tachibana, T., Tsugeki, R., Ishiguro, S. and Okada, K. (2005). Regulation of caprice transcription by myb proteins for root epidermis differentiation in arabidopsis. *Plant Cell Physiol*, **46**(6): 817-26.

Kurata, T., Ishida, T., Kawabata-Awai, C., Noguchi, M., Hattori, S., Sano, R., Nagasaka, R., Tominaga, R., Koshino-Kimura, Y., Kato, T., Sato, S., Tabata, S., Okada, K. and Wada, T. (2005). Cell-to-cell movement of the caprice protein in arabidopsis root epidermal cell differentiation. *Development*, **132**(24): 5387-98.

Kwak, S. H. and Schiefelbein, J. (2007). The role of the scrambled receptor-like kinase in patterning the arabidopsis root epidermis. *Developmental Biology*, **302**(1): 118-131.

Kwak, S. H., Shen, R. and Schiefelbein, J. (2005). Positional signaling mediated by a receptor-like kinase in arabidopsis. *Science*, **307**(5712): 1111-3.

Lee, M. M. and Schiefelbein, J. (1999). Werewolf, a myb-related protein in arabidopsis, is a position-dependent regulator of epidermal cell patterning. *Cell*, **99**(5): 473-83.

Lukowitz, W., Mayer, U. and Jurgens, G. (1996). Cytokinesis in the arabidopsis embryo involves the syntaxin-related knolle gene product. *Cell*, **84**(1): 61-71.

Masucci, J. D., Rerie, W. G., Foreman, D. R., Zhang, M., Galway, M. E., Marks, M. D. and Schiefelbein, J. W. (1996). The homeobox gene *glabra 2* is required for position-dependent cell differentiation in the root epidermis of *arabidopsis thaliana*. *Development*, **122**: 1253-1260.

Masucci, J. D. and Schiefelbein, J. W. (1996). Hormones act downstream of *ttg* and *gl2* to promote root hair outgrowth during epidermis development in the *arabidopsis* root. *Plant Cell*, **8**(9): 1505-17.

Muller, S., Han, S. and Smith, L. G. (2006). Two kinesins are involved in the spatial control of cytokinesis in arabidopsis thaliana. *Curr Biol*, **16**(9): 888-94.

Nakajima, K., Furutani, I., Tachimoto, H., Matsubara, H. and Hashimoto, T. (2004). Spiral1 encodes a plant-specific microtubule-localized protein required for directional control of rapidly expanding arabidopsis cells. *Plant Cell*, **16**(5): 1178-90.

Nakajima, K., Sena, G., Nawy, T. and Benfey, P. N. (2001). Intercellular movement of the putative transcription factor shr in root patterning. *Nature*, **413**(6853): 307-11.

Paredez, A. R., Somerville, C. R. and Ehrhardt D. W. (2006). Visualization of cellulose synthase demonstrates functional association with microtubules. *Science*, **312**: 1491-5.

Rechsteiner, M. and Rogers, S. W. (1996). Pest sequences and regulation by proteolysis. *Trends Biochem Sci*, **21**(7): 267-271.

Roudier, F., Fernandez, A. G., Fujita, M., Himmelspach, R., Borner, G. H., Schindelman, G., Song, S., Baskin, T. I., Dupree, P., Wasteneys, G. O. and Benfey, P. N. (2005). Cobra, an arabidopsis extracellular glycosyl-phosphatidyl inositol-anchored protein, specifically controls highly anisotropic expansion through its involvement in cellulose microfibril orientation. *Plant Cell*, **17**(6): 1749-63.

Ryu, K. H., Kang, Y. H., Park, Y. H., Hwang, I., Schiefelbein, J. and Lee, M. M. (2005). The werewolf myb protein directly regulates caprice transcription during cell fate specification in the arabidopsis root epidermis. *Development*, **132**(21): 4765-75.

Schellmann, S., Schnittger, A., Kirik, V., Wada, T., Okada, K., Beermann, A., Thumfahrt, J., Jurgens, G. and Hulskamp, M. (2002). Triptychon and caprice mediate lateral inhibition during trichome and root hair patterning in arabidopsis. *Embo J*, **21**(19): 5036-46.

Scheres, B., Wolkenfelt, H., Willemsen, V., Terlouw, M., Lawson, E., Dean, C. and Weisbeek, P. (1994). Embryonic origin of the arabidopsis primary root and root meristem initials. *Development*, **120**(9): 2475-2487.

Schneitz, K., Hulskamp, M., Kopczak, S. D. and Pruitt, R. E. (1997). Dissection of sexual organ ontogenesis: A genetic analysis of ovule development in arabidopsis thaliana. *Development*, **124**(7): 1367-76.

Sena, G., Jung, J. W. and Benfey, P. N. (2004). A broad competence to respond to short root revealed by tissue-specific ectopic expression. *Development*, **131**(12): 2817-26.

Sessions, A., Weigel, D. and Yanofsky, M. F. (1999). The arabidopsis thaliana meristem layer 1 promoter specifies epidermal expression in meristems and young primordia. *The Plant Journal*, **20**(2): 259-263.

Shiu, S. H. and Bleecker, A. B. (2001). Plant receptor-like kinase gene family: Diversity, function, and signaling. *Sci STKE*, **113**: RE22.

Shoji, T., Narita, N. N., Hayashi, K., Asada, J., Hamada, T., Sonobe, S., Nakajima, K. and Hashimoto, T. (2004). Plant-specific microtubule-associated protein spiral2 is required for anisotropic growth in arabidopsis. *Plant Physiol*, **136**(4): 3933-44.

Smith, L. G. (2001). Plant cell division: Building walls in the right places. *Nat Rev Mol Cell Biol*, **2**(1): 33-9.

Smith, L. G., Hake, S. and Sylvester, A. W. (1996). The tangled-1 mutation alters cell division orientations throughout maize leaf development without altering leaf shape. *Development*, **122**(2): 481-9.

Thitamadee, S., Tuchihara, K. and Hashimoto, T. (2002). Microtubule basis for left-handed helical growth in arabidopsis. **417**(6885): 193-196.

van den Berg, C., Willemsen, V., Hage, W., Weisbeek, P. and Scheres, B. (1995). Cell fate in *arabidopsis* root meristem determined by directional signaling. *Nature*, **378**: 62-65.

Wada, T., Kurata, T., Tominaga, R., Koshino-Kimura, Y., Tachibana, T., Goto, K., Marks, M. D., Shimura, Y. and Okada, K. (2002). Role of a positive regulator of root hair development, caprice, in arabidopsis root epidermal cell differentiation. *Development*, **129**(23): 5409-19.

Wada, T., Tachibana, T., Shimura, Y. and Okada, K. (1997). Epidermal cell differentiation in *arabidopsis* determined by a myb homolog, *cpc*. *Science*, **277**: 1113-1116.

Waizenegger, I., Lukowitz, W., Assaad, F., Schwarz, H., Jurgens, G. and Mayer, U. (2000). The arabidopsis knolle and keule genes interact to promote vesicle fusion during cytokinesis. *Curr Biol*, **10**(21): 1371-4.

Walbot, V. (1996). Sources and consequences of phenotypic and genotypic plasticity in flowering plants. *Trends in Plant Science*, **1**(1): 27-32.

Wasteneys, G. O. and Fujita, M. (2006). Establishing and maintaining axial growth: Wall mechanical properties and the cytoskeleton. *J Plant Res*, **119**(1): 5-10.

Zhang, F., Gonzalez, A., Zhao, M., Payne, C. T. and Lloyd, A. (2003). A network of redundant bhlh proteins functions in all ttg1-dependent pathways of arabidopsis. *Development*, **130**(20): 4859-69.

Chapter 2: Structure/Function analysis of STRUBBELIG

2-1 INTRODUCTION

In multicellular organisms, a harmonious development relies on communication between cells. Cells should receive the exact amount and duration of signal at correct time to achieve its fate. Cell communication is achieved thanks to receptors. Receptors perceive signals from neighboring cells or from the environment and transduce it into the cell. In animals and plants, the most prominent of receptor group are the receptor tyrosine kinases (RTKs) and receptor-like kinases (RLKs), respectively. RTKs and RLKs form a monophyletic superfamily (van der Geer *et al.*, 1994; Shiu and Bleecker, 2001). Between plant and animal, receptor kinase present different and common biochemical properties. The main difference is the nature of the kinase domain. While animal receptors are mainly tyrosine kinases, serine/threonine kinases structure plant RLKs. Nevertheless, tyrosine and serine/threonine kinases are composed by the same domain organization and thus may have a similar mode of action (Ullrich and Schlessinger, 1990; Hubbard and Till, 2000). These two types of receptors show a sequence and structure diversity of their extracellular domain, which allows their classification (Walker, 1994; Hubbard and Till, 2000). Contrary to animals, the largest group of plant RLKs is the leucine-rich repeat receptor-like kinase family (LRR-RLK) with 216 genes out the 610 arabidopsis RLK genes (Shiu and Bleecker, 2001). The function of the plant LRR-RKLs is broad and crucial for the plant. For example, the CLAVATA1 (CLV1) LRR-RLK has a key role in the maintenance of the shoot apical meristem (SAM) stem cell population (Clark *et al.*, 1993; Clark and Meyerowitz, 1994; Clark *et al.*, 1995). While BRASSINOSTEROIDS INSENSITIVE1 (BRI1) and BRI1-ASSOCIATED RECEPTOR KINASE1 (BAK1) receptors are involved in the perception of brassinosteroids, which is a hormone promoting growth, yield and resistance to unfavorable environment conditions (Clouse *et al.*, 1996; Li *et al.*, 2002; Nam and Li, 2002; Krippach et al., 2000). Furthermore, FLAGELIN SENSITIVE2 (FLS2) mediates plant defense resistance against bacteria (Gomez-Gomez and Boller, 2000).

LRR-RLKs consist of an extracellular domain perceiving the signal. The extracellular domain is notably composed of LRR domains. A single membrane-spanning domain connects the extracellular domain to the intracellular kinase domain. Each domain presents a particular function depending on its structure.

2-1-1 The extracellular part of LRR-RLKs

2-1-1-1 LRR domains

Extracellular domain of LRR-RLKs present repetition of a conserved motif rich in leucines called leucine-rich repeat (LRR). In plants, the number of repetitions ranges from 5 to 30 (Zhao *et al.*, 2000; Li *et al.*, 2002; Nam and Li, 2002). The LRR motif is predicted to be involved in protein-protein interactions (Kobe and Deisenhofer, 1993). For the RLKs, proteins interacting with the LRR domain may be ligands or co-receptors. In plants, LRR are composed of 23-25 amino acids and the conserved sequence is LxxLxxLxLxxNxLt/sgxIpxxLGx (x, any AA, Dievart and Clark, 2004). Before the conserved asparagine of the LRR motif, the structure is made of a β sheet, while the second part of the LRR motif forms a helix. The conserved asparagine corresponds to a turn between the β sheet and the helix. The tertiary structure of LRRs shapes as a horseshoe, where the β sheet face is solvent exposed (Kajava *et al.*, 1995). The horseshoe motif constitutes the ligand receptacle (Kobe and Deisenhofer, 1993). For several characterized plants LRR-RLKs, mutant alleles affecting the LRR domains have been identified. Except for *bri1-9*, which shows a weak phenotype, these alleles (*clv1-4*, *clv1-8*, *er-103*, *er-117* and *fls2-24*,) display intermediate or strong phenotypes (Dievart and Clark, 2004); Table 2-1 lists all mutations in the different RLKs mentioned in section 2-1-1)

2-1-1-2 Cysteine pairs

One feature of LRR-RLKs is the presence of cysteine pairs flanking the LRRs. The cysteine pair, which is located before the LRRs usually follows a conserved motif through plant LRR-RLKs (CxWxGV(S/T)C, where x is any AA; *Torii and Clark, 2000). The cysteine pair located just after the LRR domain are also separated by six

or seven AAs but do not show conserved motifs. In some LRR-RLKs, only one pair of cysteines is present; either the N-teminal pair like in the SOMATIC EMBRYOGNESIS RECEPTOR1 KINASE (SERK1) or the C-terminal pair as in XA21, a receptor involved in plant–pathogen resistance (Ronald *et al.*, 1992; Torii and Clark, 2000; Shah *et al.*, 2001). These cysteines can be involved in disulfide bridges with cysteines of a protein partner and allow the formation of dimer receptor complex (Kobe and Deisenhofer, 1994). Indeed, RLKs usually form homo- or heterodimers. For instance, the receptor-like protein CLAVATA2 (CLV2) heterodimerizes with CLV1 (Jeong *et al.*, 1999). CLV1/2 possess both pairs of cysteines. Another receptor complex is BRI1 and BAK1/SERK3 (Li *et al.*, 2002; Nam and Li, 2002). The interaction takes place in endosomes and at restricted places of the plasma membrane (Russinova *et al.*, 2004). BRI1 and BAK1 present a paired cysteines in the N-terminal of the LRRs. *bri1-105* is altered at the second cysteine from the amino-terminal cysteine pairs (Noguchi *et al.*, 1999). BRI1 interaction with BAK1/SERK3 may be involved in receptor recycling (Russinova *et al.*, 2004). BRI1 also possess cysteines before the transmembrane (TM), which may participate to the formation of BRI1 homodimer involved in brassinosteroid perception (Wang *et al.*, 2005).

2-1-1-3 Other extracellular domains

In addition of the number of LRR domains, the presence of other domains specified each LRR-RLKs. BRI1 and SERK1 possess one leucine zipper domain at the N-terminal of the protein whereas BAK1 displays four of them (Li and Chory, 1997; Hecht *et al.*, 2001; Li *et al.*, 2002; Nam and Li, 2002). Leucine zipper domain constitutes a coiled-coil domain involve in dimerization (O'Shea *et al.*, 1991). Other domains can be found between LRR and the transmembrane domains. For instance, in BAK1, a proline-rich region is found while BRI1 present a stretch of AA without determinate domain including the C-terminal cysteine pair. However, changing the threonine at position 750 to isoleucine alters the brassinosteroids pathway and suggests a function of this unknown domain (Friedrichsen *et al.*, 2000).

A feature distinguishing BRI1 from the other LRR-RLKs is the separation of the LRR21 from the LRR22 by seventy AA called island (Li and Chory, 1997). Based

on phenotype obtained in alleles with missense mutation in the island (*bri1-113*, *bri1-6* and *bri1-7*, Table 2.1), its integrity is important for BRI1 function (Li and Chory, 1997; Noguchi *et al.*, 1999). Indeed, the island and LRR22 constitute the binding site of brassinolides, the ligand of BRI1 (Kinoshita *et al.*, 2005).

The main role of RLK extracellular domain is the binding of the ligand. But how does the binding of a ligand activate and induce phosphorylation of the intracellular kinase domains?

Table 2-1. Missense mutations in plant extracellular domain of LRR-RKLs

Alleles	AA changes	Localization of mutations	References
bri1-105	C69Y	Second cystein of N-terminal Cys pair	Noguchi *et al.*, 1999
clv1-4	G201E	LRR5	Clark *et al.*, 1993 and 1997
clv1-8	D295N	LRR9	Medford *et al.*, 1992
er-103	M282I	LRR10	Torii *et al.*, 1996
er-117	G489D	LRR18	Lease *et al.*, 2001
fls2-24	R318G	LRR10	Gomez-Gomez and Boller, 2000
bri1-9	S662F	LRR22	Noguchi *et al.*, 1999
bri1-113	G611E	Island	Li and Chory, 1997
bri1-7	G613S	Island	Noguchi *et al.*, 1999
bri1-6	G644D	Island	Noguchi *et al.*, 1999 Friedrichsen *et al.*, 2000
bri1-102	T750I	Extrajuxtamembrane	Friedrichsen *et al.*, 2000

2-1-2 The transmembrane domain

The transmembrane domain is mediating the transduction of a signal between the extracellular and intracellular domain. A key experiment made with two human receptor types (TβFI and TβFII) of transforming growth factor-β (TGF-β) reveals the essential role of the transmembrane domain in receptor activation (Zhu and Sizeland, 1999). The authors created chimeric receptors by exchanging the transmembrane domain of TβFI and TβFII. The chimera receptors are called TβFI-II-I and TβFII-I-II. Alone, TβFI-II-I and TβFII-I-II cannot completely rescue the lack of TβFI and TβFII, respectively. But the co-expression of the two chimeras active the receptor complex independently of the ligand and in a stronger manner than the co-expression of the wild type forms. The two transmembrane domains have a different length: 22 AA for

TβFI versus 30 AA for TβFII. The difference of length itself is not the reason of the non-activation of the TβFI-II-I and TβFII-I-II since expressed together they can response to TFG-β signaling. As receptor kinase, the transmembrane domain of TβFI/II is predicted to form a helix. The increase or decrease of AA in a transmembrane helix structure will alter the relative orientation between the extracellular and intracellular part of the receptor. In TβFI-II-I/II-I-II, the length change of the transmembrane AA disorient the intracellular part by 100° in one direction for one and by 100° in the other direction for the second. By chance, the authors created two chimeric receptors with an orientation of the intracellular parts of the receptors corresponding to their active form. The result of the experiment suggests the binding of TGF-β to TβFI/II may result in a rotation of the intracellular part through the transmembrane domain. The rotation places the kinase domain in an active configuration (Zhu and Sizeland, 1999).

No missense mutations were discovered in transmembrane domains of plant RLKs. This maybe due to its short length, which reduces the change to be hit by chemical mutagens.

2-1-3 The intracellular domain

The configurational change of intracellular domain due to the binding of the ligand mostly results in the acquisition of phosphorylation ability by the kinase domain. The kinase domain is composed of 12 subdomains named I to XI with the subdomain VI divided into subdomains VIa and VIb. Alignments between different RLKs allowed the identification of important conserved AAs of the different domains (Hanks *et al.*, 1988). In subdomain II, a change of an alanine to threonine, present in all protein kinases, result in a phenotype in *bri1-1* (Friedrichsen *et al.*, 2000); Table 2-2 lists all mutations in the different RLKs mentioned in section 2-1-3). *bri1-8* and *bri-108/bri1-112* is the consequence of a mutation in the conserved arginine in domain VIa (Noguchi *et al.*, 1999; Friedrichsen *et al.*, 2000).

Some functions could have been attributed to certain domains. The main structural features of kinase domain are sites to anchor ATP, an aspartic residue playing the role of catalytic base, a magnesium-binding site and an activation

segment. Three subdomains of the kinase are responsible for anchoring ATP: a glycine triad in the subdomain I, a lysine in the subdomain II and a glutamine in subdomain III (Knighton *et al.*, 1991; Johnson *et al.*, 1996; Huse and Kuriyan, 2002).

The activation segment/loop is located between the DFG motif of subdomain VII and APE motif of subdomain VIII. In *clv1-9* and *bri1-104*, a conserved alanine in domain VII is changed to valine and threonine, respectively (Clark *et al.*, 1997; Li and Chory, 1997; Friedrichsen *et al.*, 2000). In addition, the change of a glycine from domain VIII also alters the function of the CLV1 and BRI1 receptors (Clark *et al.*, 1993; Clark *et al.*, 1997; Li and Chory, 1997).

In subdomain IX, mutations in both highly conserved residues as in *fls2-0/fls2-17* and in non-conserved AAs as in *clv1-2*, *bri1-101* and *bri1-117/bri1-118* can also alter the function of RLKs (Leyser and Furner, 1992; Clark *et al.*, 1997; Li and Chory, 1997; Friedrichsen *et al.*, 2000).

The activation of a receptor occurs by autophosphorylation or transphosphorylation by its co-receptor. Phosphorylations either take place in the activation segment or as in the major cases outside of the kinase domain i.e. in the end of juxtamembrane or in the C-terminal region of the kinase (Nuhse *et al.*, 2004).

Table 2-2. Missense mutations in plant intracellular domain of LRR-RKLs

Alleles	AA changes	Localization of mutations	References
bri1-1	A909T	II	Friedrichsen *et al.*, 2000
bri1-8	R983N	Via	Noguchi *et al.*, 1999
bri1-108, *bri1-112*	R983W	Via	Friedrichsen *et al.*, 2000
clv1-9	A839V	VII	Clark *et al.*, 1997
bri1-104	A1031T	VII	Li and Chory, 1997 Friedrichsen *et al.*, 2000
bri1-115	G1048D	VIII	Li and Chory, 1997
clv1-1, *clv1-5*	G856D	VIII	Clark *et al.*, 1993 and 1997
clv1-2	G881E	IX	Leyser and Funer, 1992 Clark *et al.*, 1997
bri1-101	E1078K	IX	Li and Chory, 1997
bri1-117, *bri1-118*	N1139D	iX	Friedrichsen *et al.*, 2000
fls2-17, fls2-0	G1064R	IX	Gomez-Gomez and Boller, 2000

In its activated state, the kinase domain can specifically phosphorylate intracellular components and signal perception of the bound ligand at the extracellular part i.e. the information perceived by the cell.

In this chapter, the structure/function relationship of SUB was investigated. The results of the analysis show that SUB shares feature with the majority of the characterized plant LRR-RLKs but also marks differences with them. As other LRR-RLKs, SUB may form a homo- or heterodimer receptor complex. Indeed, mutation of the first cysteine of a cysteine pair leads to *sub* phenotype. As ACR4 and ACR4 receptor classes, SUB is an atypical kinase receptor. Kinase activity could not be detected through an *in vitro* kinase assays (Gifford *et al.*, 2003; Chevalier *et al.*, 2005; Cao *et al.*, 2005). Moreover, mutations in the ATP binding site of the SUB kinase domain do not affect the function of the protein. Nevertheless, *sub-4* indicates that SUB kinase domain remains important for its function. Finally, unlike *clv1*, *sub* does not present null negative dominant phenotype (Dievart *et al.*, 2003). Thus, another RLK may not be redundant to SUB function. Finally, if the L*er* alleles of *SUB* do not display a range of phenotypic severity, *sub* might be subject to natural variation.

2-2 MATERIALS AND METHODS

2-2-1 Plant work

All seed samples received from the ABRC stock center were sterilized and germinated on Murashige and Shoog agar Petri dishes (Murashige and Shook, 1962). The different steps of the seed sterilization were 5 min incubation in sodium hypochlorite, one min in 70% ethanol and rinsed four times with sterile water. The seeds were resuspended in 0.1% agarose and plated on the Petri dishes. After 8-15 days of growth in the culture room, seedlings were transferred on soil.

2-2-2 Scanning electron microscopy

Freshly opened flower buds were immersed in Jauch's fixative (70% acetone, 2% glutaraldehyde, in H2O) and fixed overnight at room temperature. The tissue was washed 10 times in 70% acetone, rehydrated through an acetone series in a cacodylate buffer 50 mM sodium cacodylate (pH 7.0; # 20840, Fluka), postfixed in 2% osmium tetroxide (# 75632, Fluka) in cacodylate buffer for 2 hours at room temperature, washed twice in cacodylate buffer for 10 min and dehydrated through an acetone series: 20%, 40%, 60% and 70%. Subsequently, critical point drying was performed, the specimens were mounted on stubs and the ovules were dissected free. The samples were visualized thanks to a JEOL JSM-5900LV scanning electron microscope.

2-2-3 Forward genetic screen

New alleles of *sub* and *sub*-like mutants (*slms*) were isolated from an EMS-mutagenized population of Arabidopsis L*er* ecotype. The M2 generation of the EMS population was obtained from Lehle Seeds (#M2E-04-06, Round Rock, TX). About 60000 M2 derived from seven different parental groups were planted in the greenhouse. Each parental group contained 8500 M2 seeds issued from approximately 1448±81 M1 seeds. We received and screened the parental group no. 30-36 of the batch no. 99N. During the experiment the different parental groups were renamed A-F and H.

2-2-4 Reverse genetic approaches

2-2-4-1 T-DNA insertion lines

Three T-DNA insertion lines in *SUB* were ordered. One SALK line, SALK_011495 was obtained from TAIR (www.arabidopsis.org, Alonso *et al.*, 2003), one line from the SAIL collection (GARLIC_1158_D09) from the Torrey Mesa Research Institute (San

Diego, US; Sessions et al., 2002) and one line from the collection of the university of Wisconsin-Madison, (a gift from Frans Tax; (Sussman *et al.*, 2000)). The SALK and SAIL T-DNA insertion lines have a C*ol* background where as the T-DNA insertion from the Wisconsin-Madison University has a Wassilewskija (WS-2) background. The primers used to characterize the T-DNA insertions lines are summarized in Table 2-3.

2-2-4-2 TILLING

The targeting induced local lesions in genomes (TILLING) enable to find EMS-induced mutations in a gene of interest (Till *et al.*, 2003).

Interesting isolated lines by Arabidopsis project were ordered from the ABRC stock center. The EMS population of TILLING has a Col *er105* background (Big

Table 2-3. Primers used for the characterization of *SUB* T-DNA insertion

Name of the insertion line	*sub* allele	Binary vector	Primer designation (lab primer number)	Sequence
SALK_011495	*sub-6*	prok2	RK10R (43)[a]	5'-CCTGAATTGGTGACTCAAAGCA-3'
			RK11F (44)[a]	5'-TTCACACTTTGGAGACGAAACC-3'
			LBa1 (302)[b]	
Wisconsin	*sub-8*	pD991	RK2F (26)[a]	5'-TGATTTCATTGGATACGCTCCG-3'
			RK2R (27)[a]	5'-TGGAAAGCTCTCAGTACGTGTT-3'
			JL202 (254)[b]	5'-CATTTTATAATAACGCTGCGGACA TCTAC-3'
GARLIC_115 8_D09	*sub-9*	pCSA	RK7F (36)[a]	5'-TCAGATCTCTCTCAAGCAATCG-3'
			RK7R (37)[a]	5'-ATAGATTTGGCGGTATAGGCTC-3'
			LB3 (232)[b]	5'-TAGCATCTGAATTTCATAACCAAT CTCGATACAC-3'

a are specific primers to *SUB*, b and c are specific primers to the left and right border of a T-DNA insertion, respectively.

Mama). Received seeds were coming from the M3 generation. The different lines were investigating for homozygousity via sequencing. About 500 bp were amplified around the point mutation using as template extracted genomic DNA from the different lines. PCR products were purified from agarose gel with a quickgel extraction kit (#28706 Quiagen, Hilden, Germany). PCR products were sequenced

with an Applied Biosystems 373 sequencer. The sequencing PCR were setting with the bigdye terminator v1.1 cycle sequencing kit according to the

Table 2-4. Primers used for the genotyping of TILLING lines

***sub* alleles**	**Primer designation (lab primer number)**	**Sequence**
sub-10, sub-11	RK9F (40)	5'-CTTCTGCAGTTTCGGCGATT-3'
	RK9R (41)	5'-CTGCGGAATTGTCCCTGAAA-3'
sub-12, sub-13	RK6F (34)	5'-TGCCCTGACACAGAGTTCCA-3'
	RK6R (35)	5'-CAGGACAACAAGCTCACAGG-3'
sub-14, sub-15	RK6F (34)	5'-TGCCCTGACACAGAGTTCCA-3'
	RK7F (36)	5'-TCAGATCTCTCTCAAGCAATCG-3'
sub-16	RK5F (32)	5'-CCCGCTGTGGCATTGGATAC-3'
	RK5R (33)	5'-CCACCACCATCACCACCTCT-3'
sub-17, sub-18	RK4F (30)	5'-AGAAGCTCCAATATATGACCGC-3'
	RK4R (31)	5'-CTTTTGTTGCAGTTTCTCGGGA-3'
sub-19	RK2BF (336)	5'-AACACGTACTGAGAGCTTTCCA-3'
	RK2BR (337)	5'-ATAATCGGGGAAGGGTCG-3'
sub-20	RK3F (28)	5'-GCATAACCCGCCATCTACAA-3'
	RK3R (29)	5\-AACACAGAGTGACGGCGAAT-3'

manufacturer advises (Applied biosystems, sheshire, UK). Used primers are summarizing in the Table 2-4.

2-2-5 Site-directed mutagenesis

2-2-5-1 Generation of *SUB* overexpression construct

Two different overexpression constructs were used. In the first one, SUB was fused to a triple cMYC tag and the second construct contained the cDNA of *SUB* without any tag. The full-length SUB ORF was amplified from the EST *SUBc1* (accession number: W43625) by PCR (35S_for 5'-TACTCTCGAGATGAGCTTTACAAGATGGGAAG-3' and 35S_rev 5'-GGCGTCTAGATTAGATCATATGTTGAAGATCT-3') and cloned into the *Xba*I and *Xho*I sites flanked 5' by the cauliflower mosaic virus 35S promoter and 3' with a nopaline synthase transcription termination signal (ocs3') of the pART7 vector (Gleave, 1992). The cassette 35S:SUB:*ocs3'* was introduced into the *Not*I restriction site of plant transformation vector pMLBART (Siegfried *et al.*, 1999; Chevalier *et al.*,

2005). Overexpression of the translational fusion SUB3*myc (3 cpoies of myc) were obtained by Ram Kishor Yadav by overlapping PCR approaches and cloned in PCRII Topo vector (# K4600, Invitrogen).

2-2-5-2 Generation of mutagenized variants

All mutations were generated with the help of the QuikChange XL site-directed mutagenesis kit according to the manufacturer's recommendations (#200517-5, Stratagen, Cedar Creek, Texas). The SUB cDNA cloned into pART7 described above was used as template. The sequence of the mutagenized constructs was verified by sequence analysis and the inserts were subcloned into the *Not*I site of the pMLBART

Table 2-5. Used primers for the generation SUB variants

AA change	Nucleotide changes	Primer Sequence
C57Y	TGT to TAT	5'-GCTTTTGGAGGAGACCCTTATGGAGAAAAGTGGCAAGGTG-3'
		5'-CACCTTGCCACTTTTCTCCATAAGGGTCTCCTCCAAAACG-3'
V64M	GTG to ATG	5'-GAGAAAAGTGGCAAGGTATGGTGTGTGACTCCTCA-3'
		5'-TGAGGAGTCACACACCATACCTTGCCACTTTTCTC-3'
C365-6A	TGTTGC to TGTTGC	5'-GTGTGTTACACTTTGGAGATATTACAGAAGTAAAATATATAA CCG-3'
		5'-CGGTTATATATTTTACTTCTGTAATATCTCCAAAGTGTAACA C-3'
T486A	ACC to CGC	5'-CCTCATCTTCTGCTACTGTTTTCGCCATTGCTTCACTTCAGC -3'
		5'-GCTGAAGTGAAGCAATGGCGAAAACAGTAGCAGAAGATGA GG-3'
T486E	ACC to CGA	5'-CCTCATCTTCTGCTACTGTTTTCGAAATTGCTTCACTTCAGC -3'
		5'-GCTGAAGTGAAGCAATTTCGAAAACAGTAGCAGAAGATGA GG-3'
T494A	ACA to GCA	5'-GCTTCACTTCAGCAATACGCAAATAATTTCTCAGAAGAG-3'
		5'-CTCTTCTGAGAAATTATTTGCGTATTGCTGAAGTGAAGC-3'
T494E	ACA to GAA	5'-GCTTCACTTCAGCAATACGAAAATAATTTCTCAGAAGAG-3'
		5'-CTCTTCTGAGAAATTATTTTCGTATTGCTGAAGTGAAGC-3'
G506A		5'-ATAATCGGGAAGCGTCGATTGGTAATGTCTACAGAGC-3'
		5'-GCTCTGTAGACATTACCAATCGACGCTTCCCCGATTAT-3'
K525E	AAG to AAG	5'-GGAAAGTTTCTTGCGGTGGAGAAGCTGAGCAATACCATCAAC-3'
		5'-GTTGATGGTATTGCTCAGCTTCTCCACCGCAAGAAACTTTCC-3'
E539A	GAA to GCA	5'-AGAACACAGAGTGACGGCGCATTCCTCAATCTAGTCTCC-3'
		5'-GGAGACTAGATTGAGGAATGCGCCGTCACTCTGTGTTCTG-3'
R599C	CGT to TGT	5'-AAGAAGCTCACTTGGAATGTATGTATAAATATTGCATTAGG AGCTTC-3'
		5'-GAAGCTCCTAATGCAATATTTATACATACATTCCAAGTGAG CTTCTT-3'

binary vector (Siegfried *et al.*, 1999). The primers used for site-directed mutagenesis are recapitulating in the Table 2-5.

The different mutant constructs were transformed into L*er* and *sub-1* and the transgenic T1 *sub-1* plants were selected on soil by their resistance to theherbicide BASTA. The transgenic plants, which were not rescuing *sub-1* phenotype, were analyzed for transgene expression by RT-PCR and a dCAPS approach (Neff *et al.*, 1998). PCR amplification was performed on cDNA, generated by RT-PCR from flower mRNA, using the primers Sub1dcapsF 5'-TCTCTCTTCTTTGTTTGAGTGGA-3' and Sub1dcapsR 5'-CACATAGTCAATTCTCAAATGCA-3', resulting in a band of 121 bp. After overnight digestion, the 121 bp band was digested with *Ava*II, which should result in a 101 bp and 20 bp fragment and be undigested in the case of the synthesized cDNA from *sub-1* and WT transcript, respectively.

2-3 RESULTS

To learn more about the function of SUB, the role of its different domains was investigated. To this goal, new alleles of SUB were identified by reverse and forward genetic approaches. Then, the severity of the phenotypes was analyzed to determinate the importance of the altered AA. In addition, according to the knowledge about RLKs mechanisms, the importance of certain AAs of SUB was determinated. The AA changes were allowed by site-directed mutagenesis and their capacity to rescue *sub-1* phenotype was investigated.

2-3-1 Isolation of new alleles of SUB

2-3-1-1 EMS mutagenesis

To isolate new alleles of *sub,* an EMS-mutagenized population of Arabidopsis was screened for *sub*-like mutants. Therefore all plants with a similar phenotype than *sub* were retained. Although these alleles can affect a different pathway than of SUB, there is a high probability that these mutations are either new alleles of SUB or

mutations in members of the SUB pathway. Screening of approximately 60.000 mutagenized M2 plants identified 55 *sub-like mutants* (*slms*). Complementation tests with *sub-1* shown that two *slm* alleles, *slm-14* and *slm-15* were new alleles of *SUB*. Indeed the F1 generations of the crosses between *sub-1* and the different *slms* were showing *sub* phenotype. Coming from different parental group of screened seeds, they must be different alleles of *sub* (Table 2-6). *slm-14* and *slm-15* were renamed *sub-4* and *sub-5*. NB: others *slms*, altered in gene candidates of *SUB* pathway will not be discussed.

Table 2-6. Results from the screen of *sub*-like

Parental group	Number of isolated *slms*	Origin of the new *sub* alleles
A	2	-
B	27	-
C	5	*slm-15*
D	1	*slm-14*
E	3	-
F	5	-
H	10	-
Unknown bag	1	-

Backcrosses with Wt L*er* and analysis of the resulting F2 population indicate that each mutant was caused by a monogenic recessive mutation (Table 2-7).

To identify the molecular lesion, *SUB* coding region of these two new alleles were sequenced. After sequencing, a single point mutation was found in *SUB* (Table 2-8). All the point mutations were GC to AT changes, consistent with the mode action of EMS (Koornneef *et al.*, 1982). With a mutation of the 288th residue (glutamic acid) to a stop codon in the region coding for the extracellular part of SUB, predicted sub-5 is 49 AA shorter than sub-2 and is not really informative. In contrast, *sub-4* constitute our first *sub* allele affecting the intracellular part, more precisely the kinase domain of SUB. The arginine at position 599 in the subdomain VIa is replaced by a cysteine.

Table 2-7. Analysis of segregation of *sub* mutant with L*er*

Cross	F2 Segregation [L*er*]	[*sub*]	Plant total	Null hypothesis	χ^2; <P<
L*er*sub-4*	103	32	135	3:1	0,0359; 0,10-0,25
L*er*sub-5*	110	34	160	3:1	0,8896; 0,50-0,75

Segregation data was evaluated with chi-square analysis (χ^2) using the null hypothesis indicated. Chi-square values and probabilities (P) are indicated.

Table 2-8. Recapitulation of *SUB* new alleles

Alleles	Altered base	Gene localization	AA change	Affected protein domain
sub-4	CGT 3405 TGT	Exon 12	R599C	kinase VIa
sub-5	CAA 2286 TAA	Exon 10	G288*	PRR

PRR: proline-rich region

2-3-1-2 TILLING

Other alleles with point mutations in *SUB* were obtained by a TILLING approach (Till *et al.,* 2003). Briefly, the identification of mutation in a gene is based on PCR and digestion of the PCR product using CELI, a member of the S1 nuclease family. CELI enzyme cleaves all DNA mismatches (Oleykowski *et al.*, 1998). To identify mutations in *SUB*, screens were realized by the Arabidopsis TILLING project (ATP from the Seattle TILLING project, http://tilling.fhcrc.org:9366/home.html). During one screen, the Arabidopsis TILLING project can screen for mutations within 1,5 kb of genomic region. So three different screens were performed on *SUB* to obtain mutations in the LRRs region, proline-rich region, transmembrane and the kinase domain (Purple lines in Figure 2-1). From these three screens, twenty-six lines displaying a nucleotide change in *SUB* were isolated. In eight of the lines, the altered nucleotides are localized in *SUB* introns (Figure 2-1). *SUB* introns do not contain any necessary regulatory elements since *sub-1* could be rescued by the transformation of the *SUB* cDNA (see below). So, these eight lines, as well as seven lines with a nucleotide change leading to the same AA were not further analyzed.

Finally, eleven lines carried point mutations in *SUB* exons leading to and altered AA sequences (Figure 2-2). The study was carried on them. These lines were renamed *sub-10* to *sub-20* and the phenotype of those alleles was assessed. A *sub*

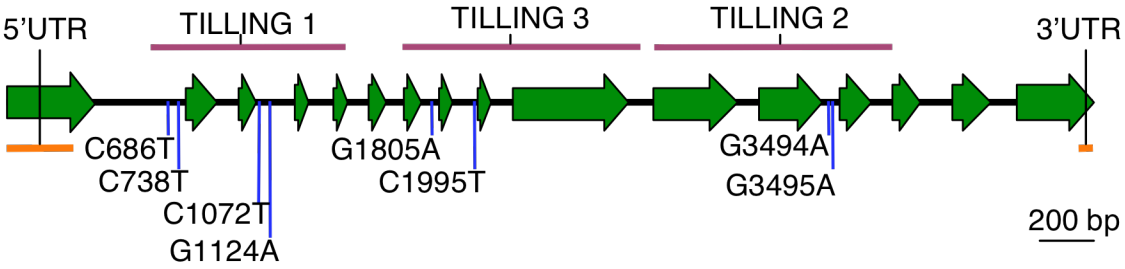

Figure 2-1. Distribution of the TILLING affected in *SUB* introns. The scheme represent *SUB* gene with its exons repartition (green arrows). Orange lines show 5' UTR and 3' UTR. The purple lines show the 3 regions where TILLING screen were performed. Blue lines indicate the different TILLING lines found in *SUB* introns. They are named by the position and nature of the change.

phenotype was observed in two different lines only. These two lines are *sub-10* and *sub-16* (Figure 2-3). *sub-10* is affected in the first cysteine of the cysteine pairs located upstream of the LRRs. *sub-16* displays a mutation in the transmembrane in the 357th codon, a glycine is changed in serine.

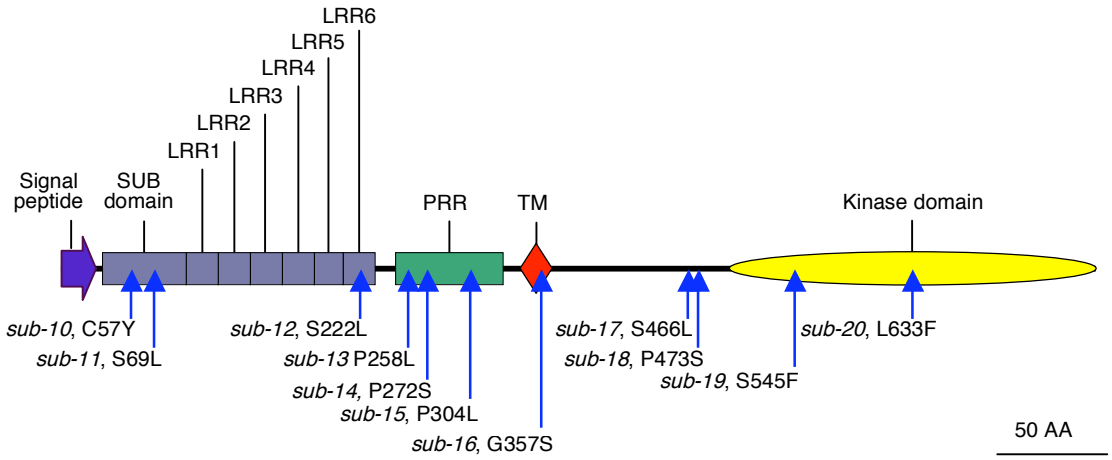

Figure 2-2. Distribution of the TILLING affected in the AA sequence of SUB. The SUB protein is represented with its different structural domains. Arrows show the different TILLING lines disturbing the AA sequence of SUB. The lines are named by *sub* alleles and their AA change. LRR: leucine riche region, PRR: proline rich region, TM: transmembrane domain.

2-3-1-3 Characterization of T-DNA lines

Three T-DNA insertion lines in *SUB* were obtained from different Arabidopsis insertion mutant collections. Two lines are in the Columbia (Col) background

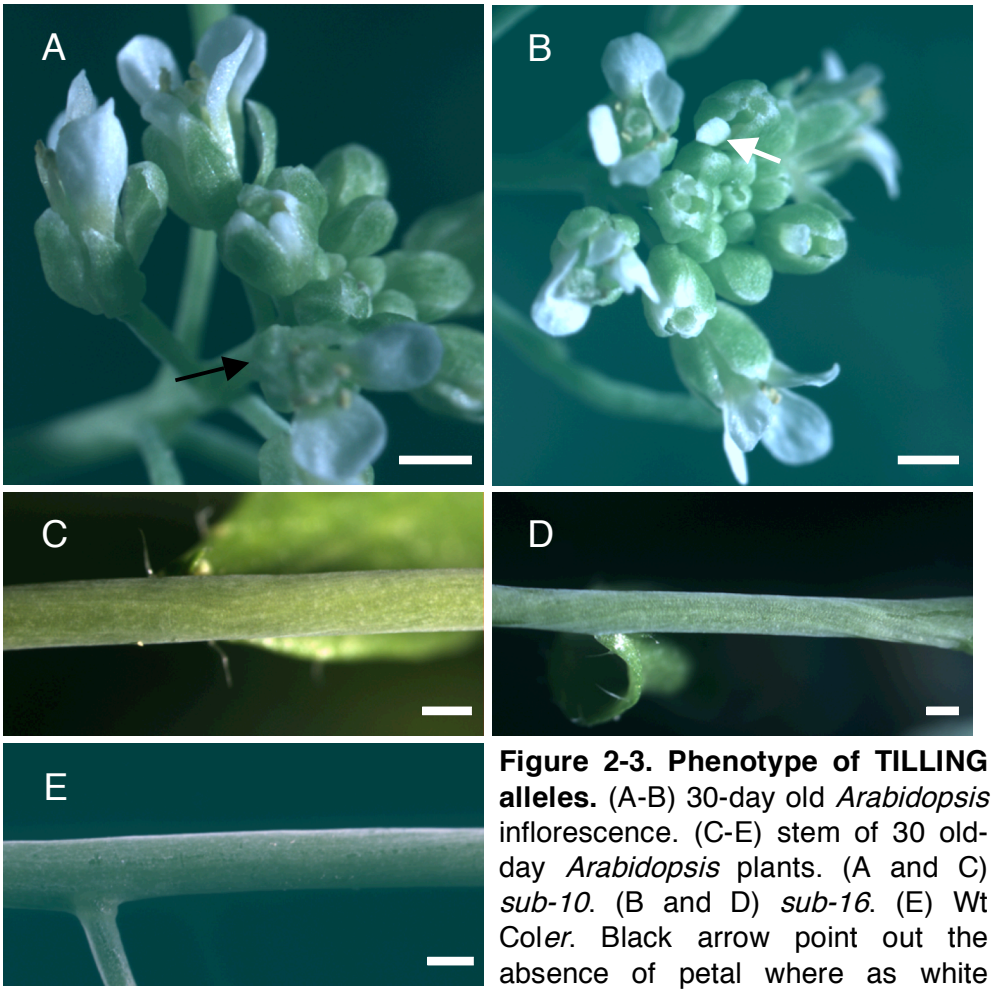

Figure 2-3. Phenotype of TILLING alleles. (A-B) 30-day old *Arabidopsis* inflorescence. (C-E) stem of 30 old-day *Arabidopsis* plants. (A and C) *sub-10*. (B and D) *sub-16*. (E) Wt Col*er*. Black arrow point out the absence of petal where as white arrow show twisted petal. Scale bar: (A-E), 1mm.

(SALK_011495 and GARLIC_1158_D09) and were renamed *sub-6* and *sub-9*, respectively. The third line has a Wassilewskija (WS-2) background and corresponds to the eighth allele of *sub* (*sub-8)*. The amplification and sequencing of genomic fragments containing a border of the insertion and a piece of *SUB* gene, allowed the localization of the insertions in *SUB*. The results are presented in Figure 2-4. *sub-6* displays the T-DNA insertion in intron 1. Translation of *sub-6* will lead to the synthesis of the first 4 AAs apart the sequence signal and can probably be considered as a null allele. T-DNA insertions in *sub-9* and *sub-8* are located in exons. In *sub-9*, conceptual translation results in a 202 AAs protein composed of the 195 first AAs of SUB and 7 new AAs. Structurally, it means that the SUB domain, the fourth first LRRs and the beginning of the fifth LRR are translated. The last T-DNA insertion line *sub-8,* carries the insertion at the end of the activation loop of the kinase domain. The

glutamine of the subdomain VII APE motif is replaced by an alanine, which then followed by 47 new AAs.

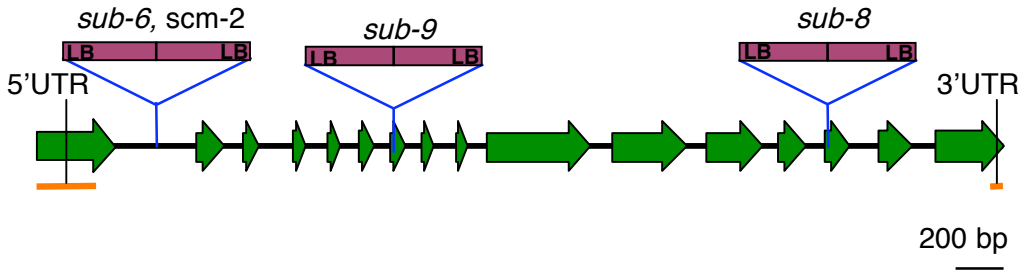

Figure 2-4. Distribution of T-DNA insertion in *SUB*. The scheme represent *SUB* gene with its exon repartition (green arrows). Orange lines show 5' UTR and 3' UTR. Purple rectangulars represent T-DNA insertions with their orientation: LB, left border, RB, right border. *sub-6*, *sub-9* and *sub-8* are a tandem T-DNA insert in a head-to-head orientation.

2-3-2 Phenotypic analysis of *sub* alleles

2-3-2-1 Comparison of *sub* phenotype in L*er* background

To establish a relation between five different point mutation alleles and the function of SUB, a detailed phenotypic analysis was performed. The five chosen alleles are *sub-1* to *sub-5*. They are all coming from a L*er* ecotype and been subjected to three backcrosses. TILLING point mutation alleles were not considered for the analysis. Backcrosses are still in progress to change their Col to L*er* background to eliminate additional mutations. The strength of the different alleles phenotype was evaluated by measuring the plant height, floral organ number and by determining abnormalities of floral organs and ovules. The twisted stem phenotype of *sub* was not analyzed due to the difficulty to estimate its degree of severity.

2-3-2-1-1 Height of the different *sub* alleles

The height of 8-week old plants was measured from the rosette leaves to the apex of the main inflorescence. The results are listed in Table 2-10. The height of *sub* is about fifty percent smaller than WT. Nevertheless no differences are observed between the different alleles of *sub*.

Table 2-10. Height of *sub* alleles

	Mean±SD	T value
L*er*	27±3,4	
sub-1	12,9±3,1	14,13
sub-2	13,3±2,9	14,19
sub-3	13,6±2,4	14,22
sub-4	15,5±1,8	14,09
sub-5	nd	

The data are given in cm. The T statistic values refer to two-tailed Student's t-tests involving Wt and the respective mutant. Degrees of freedom = (N_{Ler} + N_{sub})-2 and P < 0.001.

2-3-2-1-2 Analysis of floral organs in *sub*

Flowers from stage 13 to 15 were used (stage according to Smyth *et al.*, 1990). In L*er* wild type flowers of Arabidopsis are composed of four sepals, four petals, five or six stamens and two fused carpels. In *sub* alleles, it also possible to observe flowers with a calyx or/and a corolla of three or five elements, an androecium of four stamens and the gynoecium was sometimes composed of two carpels fused with a carpel fragment at the distal extremity. Table 2-11 shows the average and standard deviation of the different floral organs of the analyzed alleles. These two

Table 2-11. Number of floral organ in 30-days-old *sub* plants

Genotype	Sepals	Petals	Stamen	Carpels	N
L*er*	4,1 ± 0,3	4,1 ± 0,3	5,6 ± 0,5	2	50
sub-1	4,0 ± 0,4	3,6 ± 0,7 t:3,9284	5,1 ± 0,6 t:4,1295	2,0 ± 0,2	100
sub-2	4,0 ± 0,5	3,9 ± 0,6	5,5 ± 0,7	2,1 ± 0,3	100
sub-3	4,0 ± 0,6	3,7 ± 0,8	5,4 ± 0,8	2	38
sub-4	4,0 ± 0,4	3,6 ± 0,7 t:4,8276	5,5 ± 0,6	2,0 ± 0,2	100
sub-5	4,0 ± 0,5	3,8 ± 0,6 t:3,3296	5,3 ± 0,7	2,1 ± 0,2	100

The mean ± SD is shown. The t statistic values refer to two-tailed Student's t-tests involving Wt and the respective mutant. Degrees of freedom = (N_{Ler} + N_{sub})-2 and P < 0.001.

parameters were compared to the one obtained from wild type with a two-tailed Student's t-tests. *sub-1*, *sub-4* and *sub-5* show significantly different number of petals from wild type and may represent stronger alleles for this floral organ criteria.

Unexpectedly, *sub-5 and sub-2*, which both carry a stop codon in the proline rich-region, do not show similar defects in petal number.

In addition to their altered number, *sub* flowers display aberrant floral development. The defects of the different alleles of *sub* were analyzed. For each allele, frequencies of abnormalities are grouped in Table 2-12. Carpels and petals of *sub* are twisted (Figure 2-5B). In *sub-1*, 100 % of the carpels are twisting and about 70% of petals from stage 13 to 15 flowers of 30-day old show a twisting pedicel. The twisting pedicel is responsible for the “strubbelig/disheveled” appearance of *sub* flowers.

Fifty flowers were used for this analysis. Petals of *sub* can also be particularly tiny ((≤10/100, Figure 2-5D). In addition to the twisting phenotype, carpels are unfused (≤7/100, Figure 2-5E) or only partially fused at the proximal part of the carpel (≤7/100).

Moreover, floral organs can also show identity from a neighboring whorl. Sepals can be whitish as petals (≤4/100; Figure 2-5A). Petals can be greenish or show a longer pedicel with a yellow structure at the distal side, reminiscent of sepal and stamen, respectively (5≤/100). As petal can show yellow structure, stamen can present white tissue (2≤/100). A characteristic, which could have been observed in all alleles, is the fusion of anther-like tissue to the carpel (4≤/100). Other alterations of *sub* flowers are the fusion of two neighboring floral organs from the calyx and the androecium (Figure 2-5C) and smaller size (Table 2-12).